

# Thermal Expansion of Blood Vessels and Muscle Specimens Permeated with DMSO, DP6, and VS55 at Cryogenic Temperatures

YOED RABIN and JOSEPH PLITZ

Department of Mechanical Engineering, Carnegie Mellon University, Pittsburgh, PA 15213

(Received 1 December 2004; accepted 14 April 2005)

**Abstract**—As part of an ongoing effort to characterize the continuum mechanics during cryopreservation via vitrification (vitreous in Latin means glass), the current study focuses on measuring the thermal expansion of cryoprotective agents in the presence and absence of biological samples of bovine muscle and goat arteries. The cryoprotectants under investigation are 7.05M DMSO, DP6, and VS55, with permeation time of up to 48 h. This study focuses on the upper part of the cryogenic temperature range, where the cryoprotectant behaves like a liquid in all practical applications. The specific lower boundary of this range is unique to the cryoprotectant composition and to the applied cooling rate. The measurement device used in the current study is a modification of a prototype presented recently, in which modifications are made to accommodate biological samples. Based on thermal strain observations, it is concluded that the presence of tissue samples promotes crystallization (the tissue samples serve as potential nucleation sites). It is shown in this study that the thermal strain of tissue samples permeated with 7.05M DMSO and DP6 is no greater than the thermal expansion of the same cryoprotectants in the absence of tissue samples, and in some cases it is significantly less. For a given cryoprotectant in comparable thermal conditions, experiments on bovine muscle samples show significantly higher scattered data than experiments on artery samples.

**Keywords**—Cryopreservation, Thermal expansion, Bovine muscle, Blood vessels, DMSO, DP6, VS55.

## INTRODUCTION

Many mechanisms of injury are known to be involved in the process of cryopreservation of biological materials, most of which are associated with the formation of ice crystals. Plausible explanations have been offered for why ice crystals damage biological cells at the various regimes of ice crystal formation, but the outcome of crystallization is essentially the same—the extremely high certainty of cell death.<sup>9,12–14,26</sup> Cryopreservation techniques are typically focused on controlling, and ideally eliminating ice formation, frequently by introducing cryoprotective agents (or cryoprotectants) into the biomaterials.

Classical cryopreservation using relatively low concentrations of cryoprotectants, such as dimethyl sulfoxide (DMSO – one of the most commonly used cryoprotectants), have been shown to conserve many important properties of biological tissues – vascular allografts being a good example. However, the techniques developed for freezing vascular allografts are not reliable.<sup>1,11</sup> Fractures have been observed in cryopreserved arteries,<sup>7</sup> and similar observations have been made in recent studies of human arteries. In cryopreserved human internal mammary arteries and femoral arteries, both smooth muscle functions and endothelial functions were poorly-preserved.<sup>10,25</sup>

Classical cryopreservation, with low concentrations DMSO, does a reasonable job of cell preservation by preventing intracellular ice formation; but it is a very poor method for preserving tissue. Even when all major cryopreservation variables are controlled, there is a limit, largely a function of tissue volume and geometry, beyond which traditional cryopreservation methods do not work consistently. There have been several hypotheses on the mechanisms of freezing-induced injury based upon a variety of factors,<sup>8,9</sup> but it has been discovered that the disadvantages of traditional cryopreservation revolve primarily around ice formation.<sup>12–14,26</sup>

Vitrification is an alternative to conventional freezing of living biological materials (vitreous in Latin means glass). Here, ice formation is completely prevented due to the presence of high cryoprotectant concentrations that interact strongly with water. No appreciable degradation occurs over time in living matter trapped within a vitreous matrix, and vitrification is potentially applicable to all biological systems.<sup>2–5</sup> Vitrification is a relatively well understood physical process, but its application to the preservation of biological systems is not without problems, since the high cryoprotectant concentration necessary to facilitate vitrification is potentially toxic. To limit the effects of toxicity, it is necessary to use the least toxic cryoprotectant and the minimum concentration that permits glass formation (at cooling rates that are practical for bulky mammalian tissues).<sup>3–4,24</sup> While vitrification prevents the hazardous effect of ice formation, new potential mechanisms of injury

---

Address correspondence to Yoed Rabin, Department of Mechanical Engineering, Carnegie Mellon University, Pittsburgh, PA 15213. Electronic mail: rabin@cmu.edu

associated with the amorphous state have been identified and must be studied as an essential component of developing methods of cryopreservation for multi-cellular tissues. These mechanisms are related to the mechanical stress associated with the thermal expansion of the material, known as “thermomechanical stress”.<sup>6,12,15,27</sup> Thermomechanical stress is known to cause fractures during cryopreservation.

Mechanical stress in a material is related to pressure; it is the force per unit area that pulls the material apart (tensile stress), or presses it together (compressive stress). The magnitude of stress is related to the deformation of that material. Engineers define deformation, or strain, as the change in geometric size relative to the initial size. Changes in size are often much smaller than the size itself, as is the case in cryopreservation. Any material which is unrestrained will undergo a change in size (thermal strain), when subjected to a change in temperature. Materials in general—and tissues as they are cryopreserved in particular—shrink when they are brought from physiological temperature down to cryogenic temperatures (typically in the order of 0.01% per degree Celsius). The dependency of this thermal strain on temperature is largely unexplored. The main objective of the current study is to measure the thermal strain when no external forces are acting on the material.

The ratio of the change in volume, as a result of a temperature change, to the initial volume, is defined as the “volumetric thermal strain.” The “linear thermal strain” is a relative property, which is defined as one-third of the volumetric thermal strain (for simplicity, linear thermal strain and thermal strain are synonymous in this text). The term “linear thermal expansion coefficient” is an absolute thermophysical property, which is defined as the rate of change of the linear thermal strain with temperature (for simplicity, linear thermal expansion coefficient and thermal expansion are synonymous in this text).

As tissues are cryopreserved, they are externally free to strain. In practice however, it is impossible to cool a tissue of practical size uniformly; the outside surface decreases in temperature more rapidly than the inside. Each layer of tissue tends to shrink according to its local temperature, which would require that the outside tissue layers overlap the inner layers. This cannot be tolerated; therefore stresses and additional strains beyond the thermal strains, arise to make the shrinkages compatible. The outside of the tissue is forced to shrink less and the inside to shrink more. The level of stresses that must arise to accommodate the differential shrinkage depends upon the stiffness and relaxation of the material. If these stresses are too severe, they can potentially produce fractures, as has been frequently observed in cryopreservation of bulky specimens. There are methods for predicting the stresses that arise due to nonuniform changes in temperature. These methods combine mathematical analysis with data that captures (1) the thermal strain due to uniform temperature changes, and (2) the time-dependent response of stress-to-strain as a function

of temperature. Prior studies of stress development did not address realistic or optimized cryopreservation conditions in which cryoprotective agents promote vitrification. The development of such mathematical methods for cryopreservation applications is the subject matter of parallel efforts by this research group.<sup>15,17,18,20</sup> Stress development during vitrification is completely unexplored, although some phenomenological reports are available.<sup>6</sup>

As part of an ongoing effort to characterize the mechanical behavior of biological tissues and solutions at cryogenic temperatures, the current study focuses on thermal expansion measurements of tissue samples permeated with cryoprotectants. The thermal strain has been measured by Plitz and Rabin<sup>16</sup> to determine the thermal expansion of pure cryoprotectants, using an apparatus first presented by Rabin and Bell<sup>21,22</sup> and recently modified for thermal expansion measurements of tissue specimens permeated with cryoprotectants. The current study is focused on specimens permeated with high concentration of DMSO, and the cryoprotectant cocktails DP6 and VS55, which are of great interest in cryopreservation applications.<sup>22</sup> The current study is focused on the upper part of the cryogenic temperature range, where the vitrified material behaves like liquid for all practical purposes, where parallel efforts by this research group are devoted to studying thermal expansion at the lower part of the cryogenic temperature range, where the vitrified material behaves practically like solid. The boundary between the upper part and the lower part of the cryogenic temperature range is unique to the cryoprotectant composition and to the applied cooling rate. The interpretation of this boundary, based on experimental results, is further discussed in this paper.

## EXPERIMENTAL SYSTEM

A prototype of the apparatus for thermal expansion measurements used in the current study has been developed by Rabin and Bell.<sup>21</sup> This apparatus has been modified for the purpose of the current study, in order to accommodate tissue samples (Fig. 1). In broad terms, the experimental apparatus comprises an elongated enclosure, simultaneously containing a cryoprotectant and tissue samples at a cryogenic temperature, and air at room temperature. The part of this enclosure which contains the tissue samples at cryogenic temperatures is the cooling chamber. The part of the enclosure which contains air, and kept at room temperature, is the pressure tube (Tube A in Fig. 1). The pressure tube and the cooling chamber are connected through a flexible tube, filled with the same cryoprotectant which is contained in the cooling chamber (Tube B in Fig. 1). During experimentation, the volume change of the cryoprotectant within this flexible tube is negligible compared with the overall volume change of the cooling chamber.

This experimental apparatus can only be used at the upper part of the cryogenic temperature range, where the

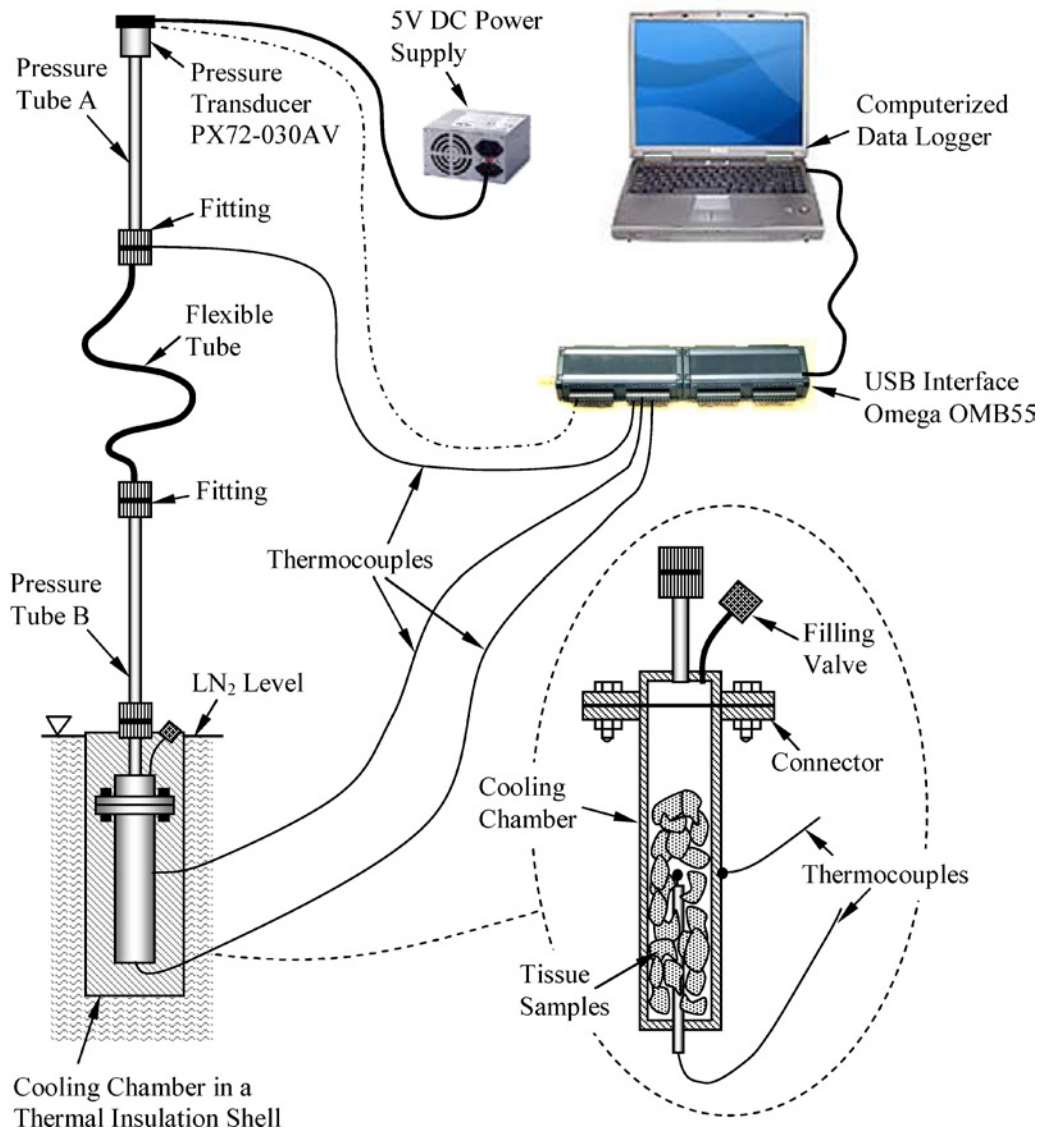


**FIGURE 1.** Schematic illustration of the experimental apparatus. The volume of the cooling chamber is 3 ml, and its inner diameter is 9 mm.

cryoprotectant behaves like a relatively low viscous fluid. Each cryoprotectant has a unique threshold below which the current apparatus will not provide accurate measurements. This threshold is either at the onset of crystallization, or at temperatures below which the viscosity of the cryoprotectant reaches values which are too high. Examples for this threshold are given in the discussion section of the current report.

The size of cooling chamber presented in Ref.<sup>21</sup> was reduced from 11.1 to 3 ml, for the purpose of the current study, in order to allow for the higher cooling rates necessary for vitrification (i.e., glass formation). The modified diameter of the cooling chamber is 9 mm, which is deemed small enough to maintain close-to-uniform temperature distribution, while cooling at the relevant high cooling rates.

This diameter is large enough to work with tissue samples, as described in the materials and methods section below. Experimental verification of close-to-uniform temperature distribution is discussed below (in the context of Fig. 3). Another modification of the new chamber is to construct it in two parts, joined by the “connector” illustrated in Fig. 1, which is essentially a miniature flange. This connector is added to allow for placing tissue samples in the chamber, as described below. Finally, the modified cooling chamber is fabricated from brass, unlike the original chamber, which was copper.

The temperature control of the cooling chamber is achieved by passive means. For cooling, the chamber is placed in the thermal insulation shell and immersed in liquid nitrogen (Fig. 1). The thickness of the thermal insulation

shell dictates the cooling rate. Rewarming is achieved by placing the cooling chamber with its insulation shell in free air at room temperature. These rewarming rates were found to be adequate for the purpose of the current study. This passive control is consistent with passive control of cryopreservation applications.

#### *Thermal Expansion of Cryoprotectants*

Data analysis of a typical experiment is performed as follows. The cooling chamber temperature and the corresponding air pressure are tabulated at 2 s intervals. For each point in time,  $t_i$ , the pressure difference is calculated:

$$\Delta P_i = P_i - P_0 \quad (1)$$

where  $P_0$  is the initial pressure (about 101 kPa). The representative sample temperature at time  $t_i$  is the numerical average of the temperature values measured at the center of the cooling chamber and at the cooling chamber wall (Fig. 1).

Next, the pressure difference  $\Delta P_i$  is converted into volume change  $\Delta V_i$  using a calibration curve. The calibration curve was prepared by connecting a micro-syringe to the pressure tube A, substituting the cooling chamber, and measuring the pressure versus displacement relationship (see Ref.<sup>21</sup> for more detail). During experimentation, the measured value of  $\Delta V_i$  includes both the thermal expansion of the cooling chamber and the thermal expansion of the material contained in the cooling chamber, which includes the cryoprotectant solution and the tissue samples. Data analysis of a cryoprotectant with no tissue samples is described first. In this case, the thermal strain of the material contained in the cooling chamber is calculated by:

$$\varepsilon_i = \frac{1}{3} \frac{(\Delta V_i + \Delta V_{\text{brass},i})}{V_0} \quad (2)$$

where  $\Delta V_{\text{brass},i}$  is the volume expansion of the brass cooling chamber from an initial temperature  $T_0$  to temperature  $T_i$ , and where  $V_0$  is the initial volume of the cooling chamber. The change in cooling chamber volume is calculated by:

$$\Delta V_{\text{brass},i} = 3V_0 \int_{T_0}^{T_i} \beta_{\text{brass}} dT \quad (3)$$

where  $\beta_{\text{brass}}$  is the thermal expansion coefficient of brass.

Next, the thermal strain data, Eq. (2), is represented by a polynomial approximation, based on a least-square approximation technique. Finally, the thermal expansion coefficient of the tissue sample is calculated by:

$$\beta = \frac{\partial \hat{\varepsilon}}{\partial T} \quad (4)$$

where  $\hat{\varepsilon}$  is the polynomial approximation of the thermal strain based on all the  $\varepsilon_i$  data.

While the thermal expansion coefficient,  $\beta$ , is an intrinsic property, independent of the technique of measurement, the thermal strain,  $\varepsilon$ , is an integral property (the integral of the

thermal expansion coefficient with respect to temperature), which is dependent on the initial conditions, or a reference point. A variation of initial temperature in the range of  $\pm 2^\circ\text{C}$ , and a variation of initial pressure in the range of  $\pm 1.4$  Pa, are typical between consecutive experiments in the experimental apparatus. In order to increase the statistical significance of the approximation of  $\hat{\varepsilon}$ , data analysis is based on  $n$  separate experiments in similar conditions. Since each experiment starts with slightly different initial conditions, the approximation of  $\hat{\varepsilon}_j$  from a specific experiment  $j$  ( $j = 1, \dots, n$ ) may need to be shifted in  $\varepsilon$  direction on the  $\varepsilon - T$  plane, so that sets of results from different experiments closely overlap. For this purpose, the approximation  $\hat{\varepsilon}_k$  ( $k = j, j = 1, \dots, n$ ) is arbitrarily selected as a reference. Next, an approximation of a second experiment is selected  $\hat{\varepsilon}_j$  ( $j \neq k, j = 1, \dots, n$ ), and all data points are shifted by a constant value  $\Delta \hat{\varepsilon}_j$  in order to minimize  $F_j$ , which is defined as:

$$F_j = \sum_i [\hat{\varepsilon}_k - (\hat{\varepsilon}_j - \Delta \hat{\varepsilon}_j)]^2 \quad (5)$$

This process is repeated for the entire set of experiments ( $j \neq k, j = 1, \dots, n$ ), where each experiment requires a different value of  $\Delta \hat{\varepsilon}_j$ . Finally, a polynomial approximation  $\hat{\varepsilon}$  is calculated based on all shifted experimental data from all the  $n$  experiments combined.

#### *Thermal Expansion of Tissue Samples*

When tissue samples are immersed in the cryoprotectant, the thermal strain of the material contained in the cooling chamber is:

$$\varepsilon_i = \frac{1}{3} \frac{(\Delta V_{\text{CPA}} + \Delta V_{\text{tissue}})}{V_0} = (1-x)\varepsilon_{\text{CPA}} + x\varepsilon_{\text{tissue}} \quad (6)$$

where  $x$  is the ratio of the overall tissue samples volume to the cooling chamber volume, and  $\varepsilon_{\text{CPA}}$  is the thermal strain of the cryoprotectant in the absence of biological samples. It follows that:

$$\varepsilon_{\text{tissue}} = \frac{\varepsilon_i - (1-x)\varepsilon_{\text{CPA}}}{x} \quad (7)$$

It is emphasized that the thermal strain (or expansion) of the cryoprotectant is measured first, in the absence of tissue sample, following the analysis presented by Eqs. (1)–(5), and only then is the thermal expansion of tissues measured, as presented by Eq. (7).

## MATERIALS AND METHODS

All experiments were performed at the Biothermal Technology Laboratory of the Department of Mechanical Engineering at Carnegie Mellon University. Tissue sample experiments were carried out in accordance with the approval of the Institutional Animal Care and Use Committee of Carnegie Mellon University.

The current study includes thermal expansion measurements of bovine muscle samples and goat artery samples, permeated with the cryoprotectant 7.05 M DMSO, and permeated with the cryoprotectant cocktails DP6 and VS55. DP6 is a cocktail of 234.4 g/l DMSO (3 M), 228.3 g/l propylene glycol (3 M), and 2.4 g/l HEPES in EuroCollins solution. VS55 is a cocktail of 242.14 g/l DMSO (3.1 M), 168.38 g/l propylene glycol (2.2 M), 139.56 g/l formamide (3.1 M), and 2.4 g/l HEPES in EuroCollins solution. The two cocktails are similar, excepting the exclusion of formamide from DP6. In return, the DP6 contains a higher concentration of propylene glycol. DMSO is one of the most commonly studied cryoprotectants, which is also an ingredient in both cocktails. 7.05 M DMSO solution contains the same overall mass of solutes as in the cocktail of VS55, where 7.05 M DMSO and VS55 were found to have similar thermal expansion in previous studies,<sup>16</sup> but 7.05 M DMSO has a much higher tendency to vitrify in comparable cooling rates.

The mixtures of DP6 and VS55 were prepared by Organ Recovery Systems, Inc. The 7.05 M DMSO solution was prepared at the Biothermal Technology Laboratory at Carnegie Mellon University, in 100 ml quantities. In preparing the solution, the solvent is added first. Next, 20 ml (or 20% of the total volume) of EuroCollins is added. Finally, distilled water is added until the desired volume of 100 ml is achieved. The water used to make the cryoprotectant solutions was cooled (frozen) once, to the liquid nitrogen boiling temperature of  $-196^{\circ}\text{C}$ , before the solutions were prepared. This precooling was performed to remove dissolved gasses from the water, as discussed in the Results and Discussion section below.

Bovine muscle samples and goat artery samples were prepared from fresh tissues donated by a local slaughterhouse (no animals were sacrificed specifically for the purpose of the current study). Goat arteries were obtained from the neck area (carotid artery), while muscle specimens were mostly obtained from the lower back area of the animal. The donated tissues were immediately cut into small segments, with typical dimensions of  $2\text{ mm} \times 2\text{ mm} \times 2\text{ mm}$  for bovine muscle segments, and typical dimensions of  $1\text{ mm} \times 2\text{ mm} \times 2\text{ mm}$  for goat artery segments (the thickness of the artery wall obtained was about 1 mm). Next, tissue samples were immersed in the various cryoprotectant solutions for permeation periods ranging between 4 to 48 h, while the samples were kept refrigerated at  $4^{\circ}\text{C}$ . Finally, tissue samples were placed in the cooling chamber, and thermal strain measurements were carried out. The numbers of experiments for each tissue type and cryoprotectant solution are listed in Table 1.

At the end of the experiments, the tissue samples and the cryoprotectant were removed from the cooling chamber. The tissue samples were further separated from the remaining cryoprotectant, and the overall weight of the tissue samples was measured. The ratio of the overall volume

of the tissue samples to the volume of the cooling chamber,  $x$ , was approximated as the ratio of the tissue sample weight to the total weight of cryoprotectant and tissue samples.

## RESULTS AND DISCUSSION

Figure 2 presents experimental results of the pressure measured in the cooling chamber as a function of temperature for three typical cases. In the relevant pressure range, the change in pressure is almost linearly dependent on the change in volume of the sample, through the calibration curve relationship described above and presented in detail in Ref.<sup>21</sup> It follows that the strain is almost linearly dependent on the pressure. The lower curve in Fig. 2(a) presents a super-cooling process of 7.05 M DMSO in the absence of tissue samples, where the pressure (proportional to the thermal strain) changes monotonically, as is to be expected from a fluid. The term “super-cooling” is used to describe material in the liquid state below its phase transition temperature range; “phase transition temperature range” describes the temperature range in which solutions and mixture undergo crystallization or melting at close-to-equilibrium thermal conditions. If the material is super-cooled to temperatures low enough, the likelihood of crystallization vanishes as a result of the dramatic elevation of viscosity with the decrease in temperature. The temperature below which the super-cooled material is considered to have an extremely high value of viscosity (typically,  $10^{13}$  poise), is known as the “glass transition temperature.” In the continuum mechanics sense, the vitrified material is considered solid below the glass transition temperature.

For consistency, the same letters are used for annotation on all curves: the letter A represents the beginning of cooling; B represents the lower temperature above which the material behaves like a fluid in the particular experiment (the lowest temperature of super-cooling); and C represents the lower temperature achieved in the particular experiment. In the experiment presented in Fig. 2(a), 7.05 M DMSO behaves like a liquid down to about  $-100^{\circ}\text{C}$ . Note that the upper boundary of the phase transition temperature range for 7.05 M DMSO is about  $-40^{\circ}\text{C}$ , while its glass transition temperature is about  $-130^{\circ}\text{C}$ .<sup>16</sup> The glass transition temperatures for DP6 and VS55 are  $-119^{\circ}\text{C}$  and  $-123^{\circ}\text{C}$ , respectively.<sup>23</sup> The cooling stage was terminated at around  $-100^{\circ}\text{C}$  due to the extremely high viscosity of the cryoprotectant, which is directly related to the extremely low likelihood of crystal formation below this temperature.

Segment A–B of the upper curve in Fig. 2(a) presents a super-cooling process of muscle samples permeated with 7.05 M DMSO. Note that this experiment started at about 1.4 kPa higher pressure than the experiment discussed above. At point B, the material contained in the cooling chamber starts to expand, which deviates from the expected volume change in a super-cooled liquid. No additional volume change is measured below  $-85^{\circ}\text{C}$  for this particular

TABLE 1. Coefficients of best-fit polynomial approximation for the linear thermal strain, approximated as  $\varepsilon = a_2 T^2 + a_1 T + a_0$ , where  $R^2$  is the quality of approximation,  $t_p$  is the permeation time,  $T_{min}$  is the temperature above which the cryoprotectant behaves like a liquid (the value range from different experiments is listed in parentheses),  $T_{max}$  is the upper temperature for best fit approximation,  $x$  is the ratio of fresh tissue volume to cooling chamber volume, and  $n$  is the number of experiments

Medium	Material	$t_p$ (h)	$a_2$	$a_1$	$a_0$	$R^2$	$T_{min}$ (°C)	$T_{max}$ (°C)	$x$	$n$
7.05 M DMSO	Pure solution	—	$5.634 \times 10^{-8}$	$2.084 \times 10^{-4}$	$-4.462 \times 10^{-3}$	0.9997	-95.8 (-99.5 ... -91.0)	20.6	0.00	4
		4	$5.574 \times 10^{-7}$	$1.637 \times 10^{-4}$	$-3.995 \times 10^{-3}$	1.0000	-48.0	22.5	0.60	1
		8	$5.392 \times 10^{-7}$	$1.620 \times 10^{-4}$	$-4.006 \times 10^{-3}$	1.0000	-48.0	22.5	0.60	1
	Bovine muscles	12	$4.103 \times 10^{-7}$	$1.945 \times 10^{-4}$	$-3.572 \times 10^{-3}$	1.0000	-58.5	21.5	0.57	1
		16	$8.170 \times 10^{-7}$	$2.288 \times 10^{-4}$	$-3.280 \times 10^{-3}$	1.0000	-59.5	20	0.50	1
		24	$1.033 \times 10^{-6}$	$2.136 \times 10^{-4}$	$-3.901 \times 10^{-3}$	0.9908	-65.3 (-73.5 ... -53.0)	19.0	0.47	4
		48	$7.578 \times 10^{-7}$	$2.215 \times 10^{-4}$	$-3.373 \times 10^{-3}$	0.9986	-58.3 (-63.5 ... -53.0)	20.3	0.52	2
	Goat arteries	48	$6.127 \times 10^{-7}$	$1.995 \times 10^{-4}$	$-4.895 \times 10^{-3}$	0.9976	-93.1 (-97.5 ... -87.5)	18.8	0.53	6
VS55	Pure solution	—	$2.012 \times 10^{-7}$	$1.841 \times 10^{-4}$	$-3.839 \times 10^{-3}$	0.9981	-77.1 (-105.5 ... -64.0)	17.5	0.00	8
	Bovine muscles	24	$-1.999 \times 10^{-7}$	$1.974 \times 10^{-4}$	$-2.170 \times 10^{-3}$	0.9999	-46.5 (-46.0 ... -47.0)	19.3	0.47	2
		48	$4.118 \times 10^{-7}$	$1.852 \times 10^{-4}$	$-2.655 \times 10^{-3}$	0.9919	-47.8 (-46.5 ... -49.0)	19.3	0.63	2
	Goat arteries	48	$9.425 \times 10^{-7}$	$2.081 \times 10^{-4}$	$-3.711 \times 10^{-3}$	0.9690	-63.6 (-82.5 ... -57.0)	19.4	0.49	8
DP6	Pure solution	—	$3.899 \times 10^{-7}$	$1.935 \times 10^{-4}$	$-4.130 \times 10^{-3}$	0.9989	-67.9 (-72.0 ... -64.2)	18.6	0.00	5
	Bovine muscles	24	$7.421 \times 10^{-7}$	$1.568 \times 10^{-4}$	$-4.213 \times 10^{-3}$	0.9905	-39.4 (-44.0 ... -35.0)	22.0	0.55	4
		48	$1.017 \times 10^{-6}$	$1.512 \times 10^{-4}$	$-4.286 \times 10^{-3}$	0.9930	-35.5 (-39.0 ... -32.5)	19.4	0.55	4
	Goat arteries	48	$1.041 \times 10^{-6}$	$1.653 \times 10^{-3}$	$-4.447 \times 10^{-3}$	0.9984	-40.5 (-43.0 ... -38.5)	19.2	0.55	6

Note. Following Eq. (4), the thermal expansion coefficient is:  $\beta = 2a_2 T + a_1$ .

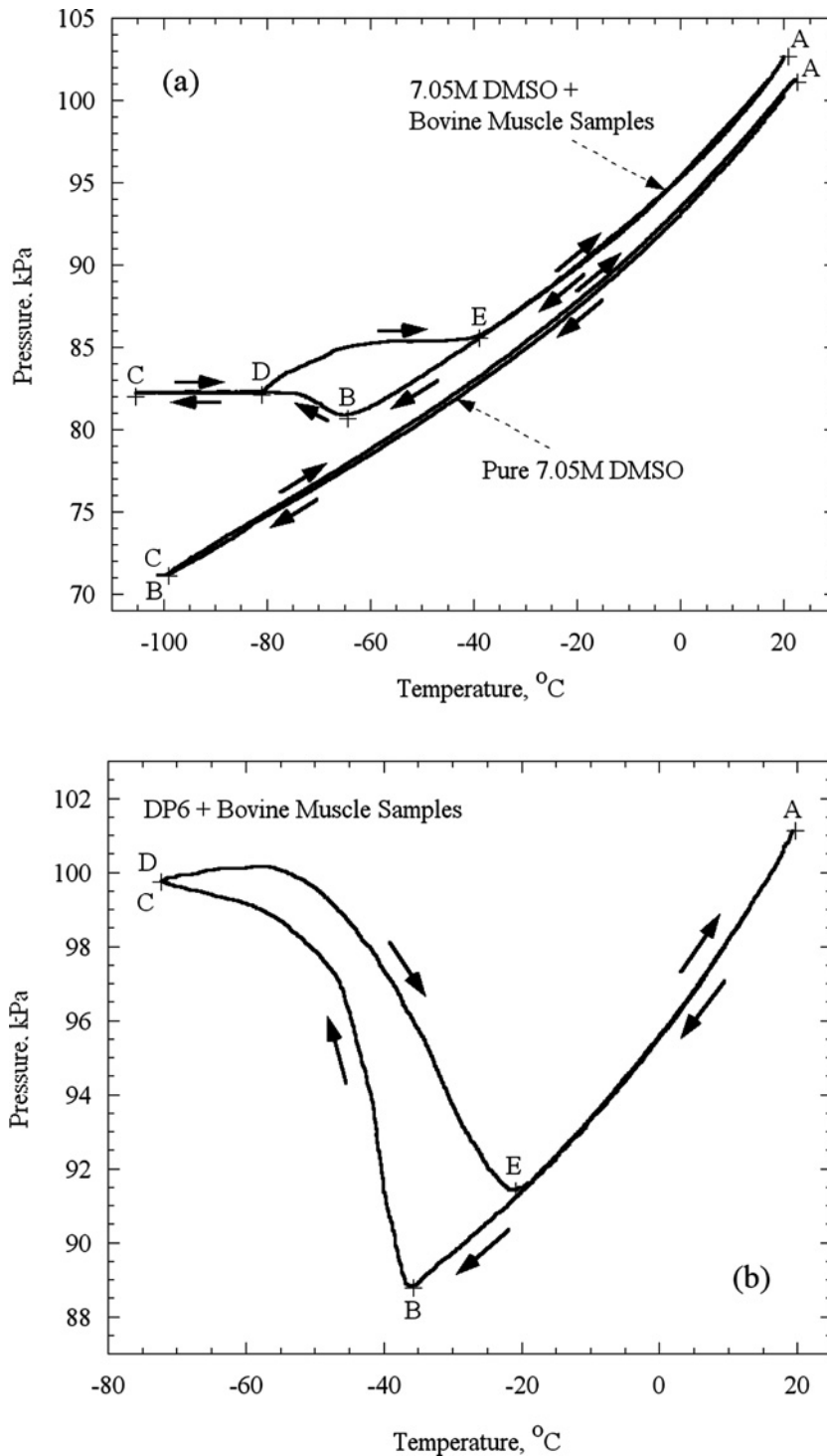


**FIGURE 2.** Experimental results of pressure as a function of temperature for three typical cases: (a) super-cooling of 7.05 M DMSO in the absence of biological samples (lower curve), devitrification of 7.05 M DMSO containing bovine muscle samples (upper curve), and (b) crystallization and melting of DP6 containing bovine muscle samples.

experiment, where—due to its high viscosity, and possibly to the presence of partial crystallization—the material cannot flow in the cooling chamber, in the typical time scale of the experiment. During rewarming, the material starts to ex-

pand at point D, which represents additional crystal growth (recrystallization) or crystal formation (devitrification) in a super-cooled liquid, up to point E, which is the upper boundary of phase transition of 7.05 M DMSO. Above point

E, the material regains its fluid behavior, and the pressure-versus-temperature curve follows the initial cooling curve (segment A–B), but in the opposite direction.

Figure 2(b) presents a pressure-versus-temperature curve of a crystallization process of bovine muscle samples permeated with DP6. In Fig. 2(b), the material ceases to behave like a liquid below point B, where a very dramatic expansion upon freezing is observed in segment B–C. Segment D–E represents melting of the solution, where complete melting of DP6 is observed above  $-22^{\circ}\text{C}$ . The temperature difference between point E and B during cooling represents the degree of super-cooling in this process. All thermal strain data reported in the current study are based on the cooling phase of each experiment, represented by segment A–B.

It is noted that the water component of the solution expands by about 9% upon freezing. Since it is well established that mammalian cells can tolerate up to 30% shrinkage during cryoprotectant addition and subsequent dehydration, it could be argued that the volume contraction of the cryoprotectant in its liquid state is insignificant compared to the volume change that the cell can tolerate. However, the rationale in this study is to model the thermal contraction of the tissue permeated with a cryoprotectant solution as a whole, for the purpose of continuum mechanical analysis, and not for the purpose of cell contraction tolerance in a fluid environment.

Figure 3(a) presents typical thermal histories of the cooling chamber for two of the experiments shown in Fig. 2, where  $T_{\text{out}}$  is the temperature at the cooling chamber wall, and  $T_{\text{in}}$  is the temperature at the center of the cooling chamber. Figure 3(b) presents the temperature difference between the center of the chamber and the chamber wall, for the same experiments. It can be seen that this temperature difference is smaller than  $3^{\circ}\text{C}$ , when crystallization is not involved in the process. This temperature difference may be more significant when crystallization is involved, due to the fact that phase transition occurs in a specific temperature range, which requires a significant change in internal energy. Hence, a significant temperature gradient is expected to develop between the cooled wall and the inwards propagating freezing front. Note that this study focuses on vitrification processes, where crystal formation is suppressed.

It can further be seen from Fig. 3 that 7.05 M DMSO has a higher tendency to super-cool than DP6, when both are cooled under similar cooling conditions, in which the cooling rate gradually increases to  $4^{\circ}\text{C}/\text{min}$  at the onset of DP6 crystallization. Note that the viscosity of the cryoprotectant increases exponentially with the decrease in temperature, which explains why the cooling rate can decrease with temperature without triggering crystallization.

The first phase of experiments in the current study included thermal strain measurements of cryoprotectants in the absence of tissue samples, as presented in Fig. 4 for:

(a) 7.05 M DMSO, (b) DP6, and (c) VS55. In Fig. 4, the symbols represent separate experimental runs, and the solid lines represent the best-fit polynomial approximation based on all experimental data for a specific cryoprotectant. The best-fit coefficients are listed in Table 1. In general, it can be seen that high repeatability is obtained for any of the solutions in which data on VS55 are somewhat more scattered than data on DP6, and the latter are somewhat more scattered than data on 7.05M DMSO. This observation is also supported by the coefficient of determination values,  $R^2$ , listed in Table 1.

Comparing the current results with results obtained in our previous study<sup>16</sup> reveals that the maximum strain difference over the entire corresponding temperature range is 2.8%, 1.3%, and 9.4%, for 7.05M DMSO, DP6, and VS55, respectively. Similarly, the maximum thermal expansion difference anywhere within corresponding temperature range is 3.7%, 3.3%, and 9.3%, for 7.05 M DMSO, DP6, and VS55, respectively. Note that the thermal strain, which is the accumulated effect (i.e., the integral) of thermal expansion, is the parameter taken into account in terms of continuum mechanics analysis. While the disagreement in thermal strain measurements for 7.05 M DMSO and DP6 is within the predicted uncertainty of the system,<sup>21</sup> the disagreement for VS55 exceeds the uncertainty in measurements by a factor of 3 (the uncertainty in the experimental system is estimated to be about  $3\%^{21}$ ). Given the high repeatability shown for VS55 in the current study, Fig. 4(c), it is concluded that this disagreement is not attributed to the measurement technique or to the experimental apparatus. It is assumed that the above difference is attributed to the specific solution under investigation. The solutions for the current study are from different batches than the solutions used in the previous study.

Figure 5 presents thermal strain measurements of artery samples permeated for 48 h with: (a) 7.05 M DMSO, (b) DP6, and (c) VS55. The symbols represent separate experimental runs, the dashed lines represent the best-fit polynomial approximation of all experimental data for a given cryoprotectant in the presence of tissue samples, and the solid lines represent thermal strain of the cryoprotectant in the absence of biological samples. A permeation time period of 48 h is deemed adequate for the small artery samples used in this study,<sup>19</sup> where the effect of varying permeation time periods is addressed below.

No indication of crystallization can be observed in Fig. 5(a), when 7.05 M DMSO is cooled down to  $-95^{\circ}\text{C}$ . The thermal strain of arteries permeated with 7.05 M DMSO is about 75% of that of a pure 7.05M DMSO solution at  $-95^{\circ}\text{C}$ . Thermal strain data on artery samples permeated with DP6 is available only down to about  $-40^{\circ}\text{C}$ , Fig. 5(b), which was found to be the onset of crystallization at the presence of tissue samples. In the absence of tissue samples, thermal strain of DP6 could be measured down to about  $-70^{\circ}\text{C}$ , Fig. 4(b). Therefore, it is concluded

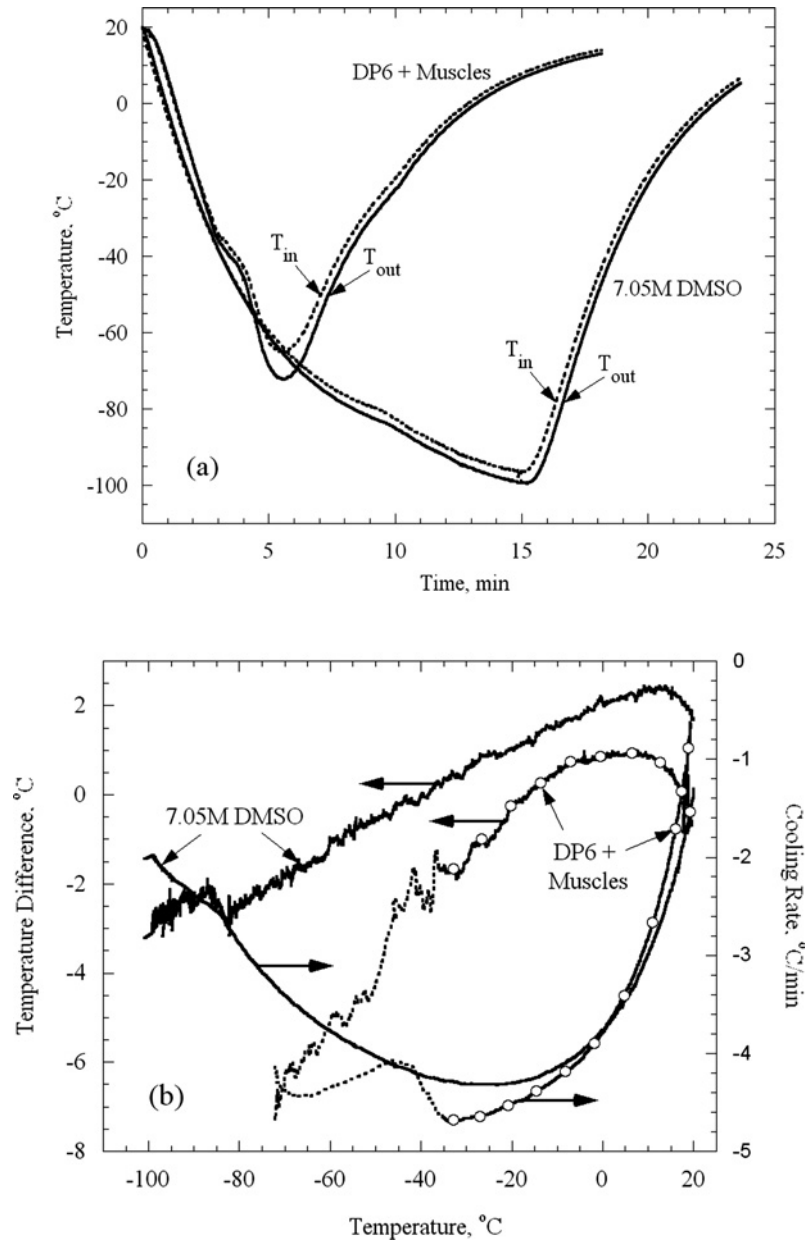


**FIGURE 3.** Thermal results of two of the experiments shown in Fig. 2: (a) thermal history, where  $T_{in}$  and  $T_{out}$  represent the inner and outer thermocouples of the cooling chamber shown in Fig. 1, and (b) maximum temperature difference and cooling rate data for the same experiments shown in Fig. 3(a). The dotted line represents data during phase transition.

that the tissue samples promote crystallization, potentially serving as nucleation sites. It is evident that the cooling rate obtained in these experiments does not permit tissue vitrification when permeated with DP6.

Thermal strain data on artery samples permeated with VS55 show significantly higher scattering than data on samples permeated with the other two cryoprotectants, Fig. 5(c). Comparable observations were made from data on bovine muscles experiments. This scattering may be an inherent effect of biological tissues permeated with the cocktail VS55, but can also be attributed to reasons for which the difference

in thermal strain between the current study and the previous study<sup>16</sup> is significant, as discussed above with regard to Fig. 4. The implication of this scattering in continuum mechanics analysis of cryopreserved tissues may be that, even if the tissue is cooled at close-to-uniform thermal conditions, mechanical stress may develop due to nonuniform thermal strain distribution. This effect, as well as other continuum mechanics effects during tissue vitrification, is the subject matter of parallel efforts by this research group.

Figure 6 presents thermal strain measurements of bovine muscle samples permeated with 7.05 M DMSO: (a) subject

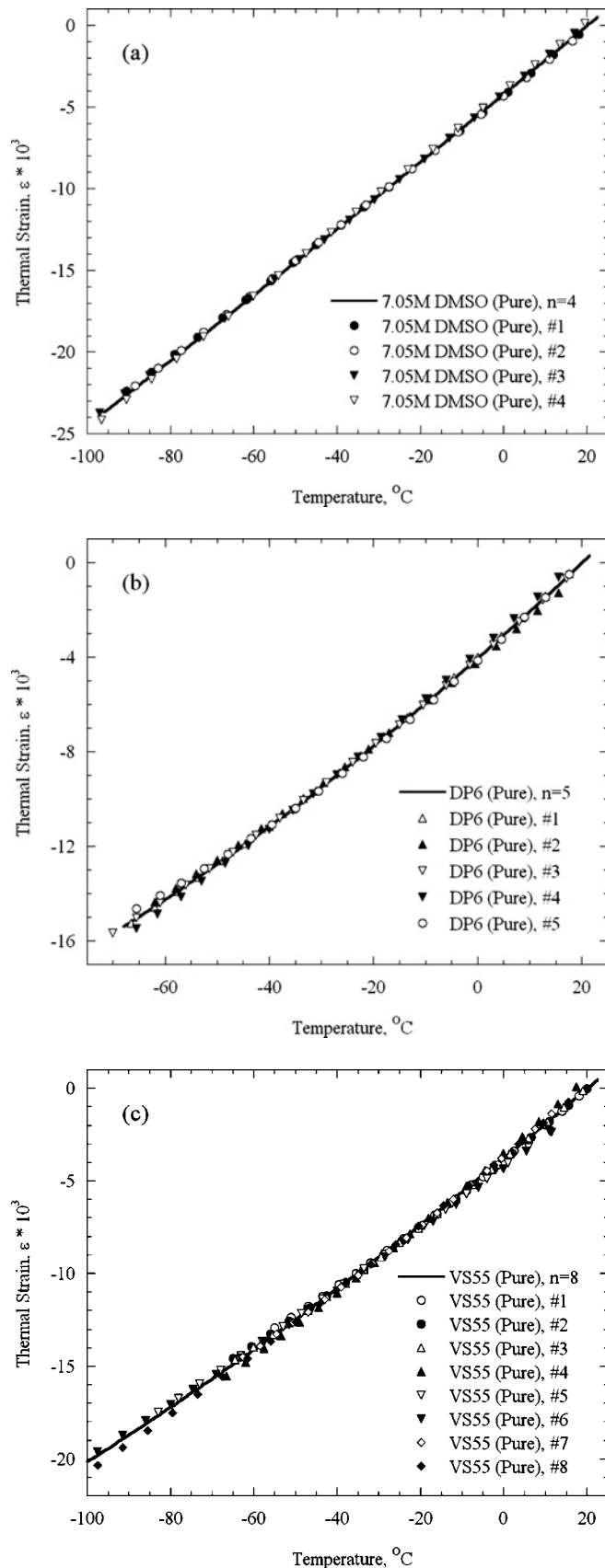


FIGURE 4. Thermal strain of the cryoprotectants: (a) 7.05 M DMSO, (b) DP6, and (c) VS55. Symbols represent separate experimental runs; solid lines represent the best-fit polynomial approximation of all experimental data. Best-fit coefficients are listed in Table 1.

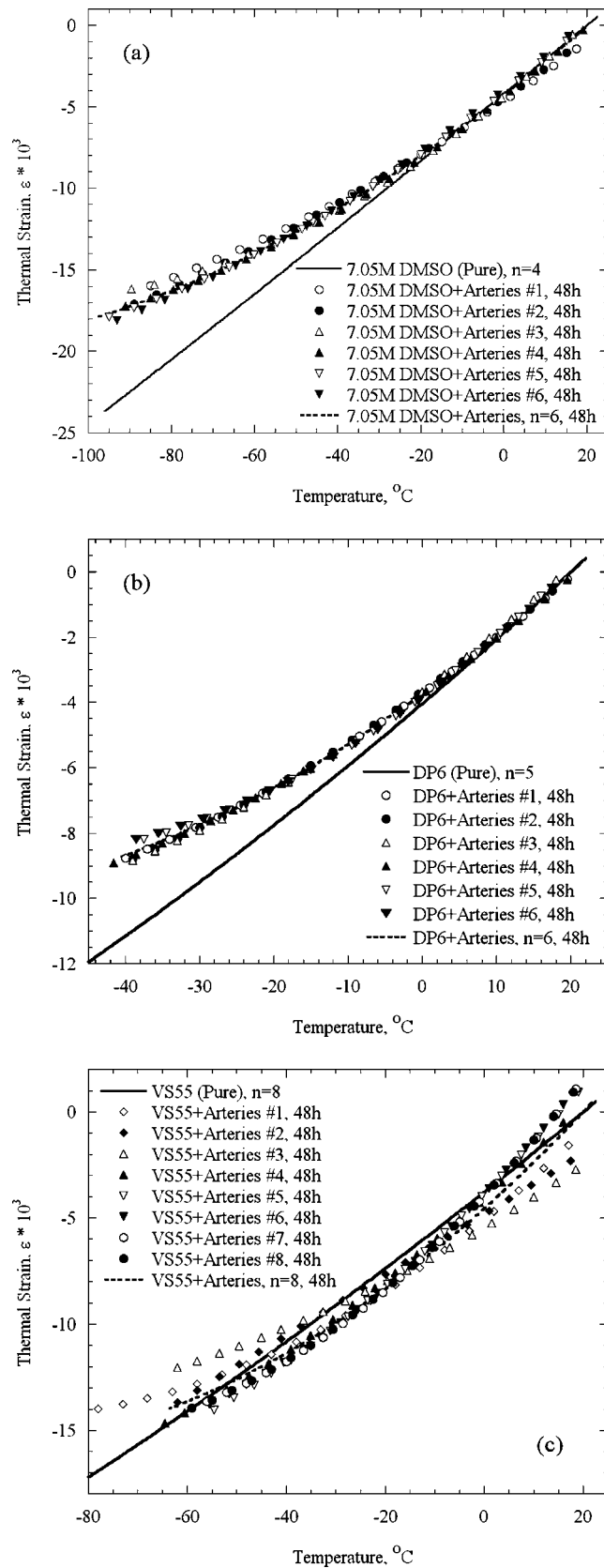


FIGURE 5. Thermal strain of artery samples permeated for 48 h with: (a) 7.05 M DMSO, (b) DP6, and (c) VS55. Symbols represent separate experimental runs; dashed lines represent best-fit polynomial approximation of all experimental data for a given cryoprotectant; solid lines represent thermal strain of the cryoprotectant in the absence of biological samples. Best-fit coefficients are listed in Table 1.

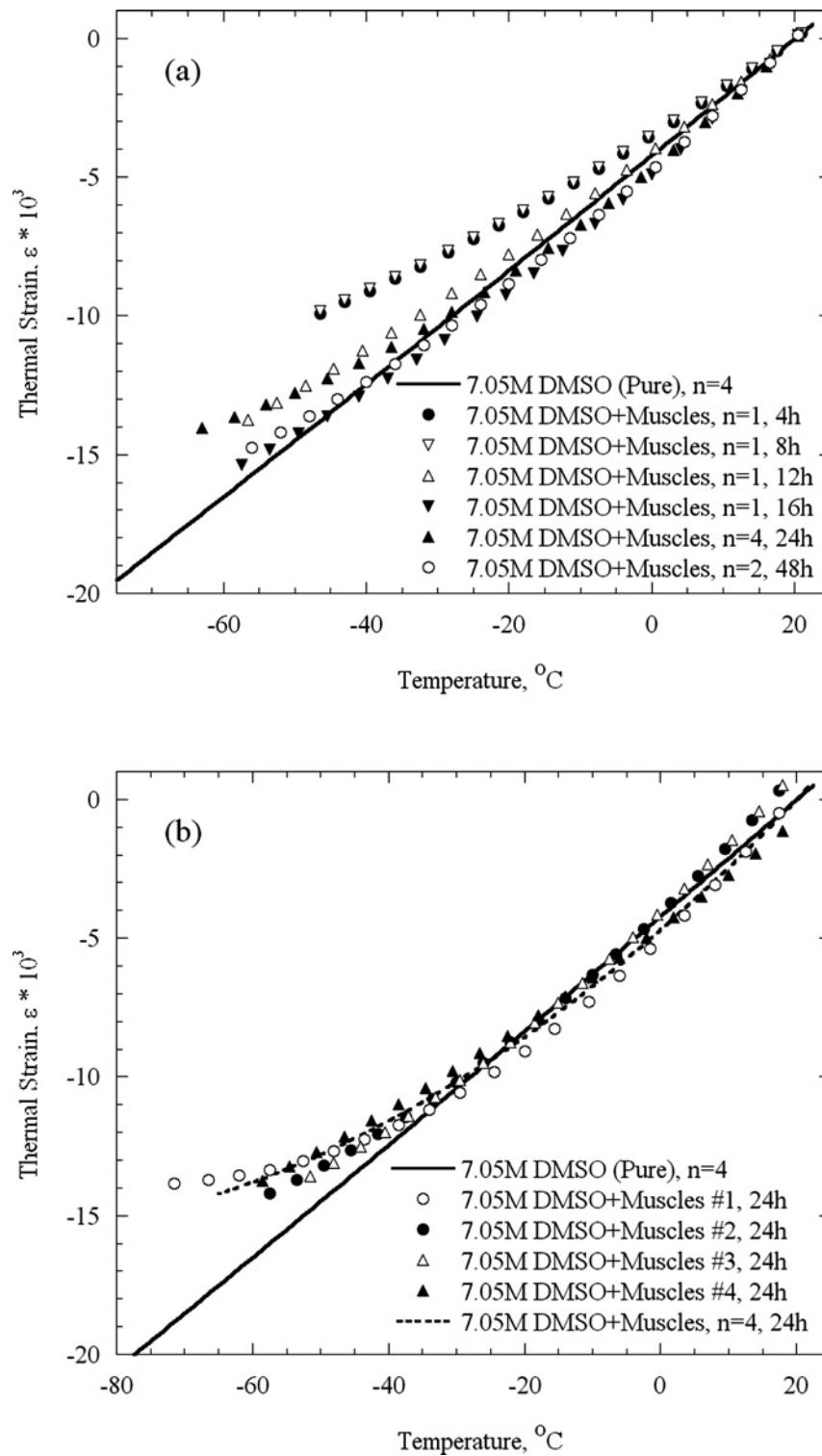


FIGURE 6. Thermal strain of bovine muscle samples permeated with 7.05 M DMSO: (a) after various permeation periods, and (b) all runs from a permeation period of 24 h. In figure (b), symbols represent separate experimental runs; dashed line represents the best-fit polynomial approximation of all experimental data; solid line represents thermal strain of the cryoprotectant in the absence of biological samples. Best-fit coefficients are listed in Table 1.

to various permeation periods, and (b) after 24 h of permeation. In general, results obtained from bovine muscle samples show higher scattering than comparable results obtained from goat artery samples. This effect is likely to be associated with the inhomogeneous nature of the muscle tissue in the small scale, related to muscle fibers, connective tissue, etc. Figure 6(b) presents the agreement of all bovine muscle experiments for 24 h of permeation. It can be seen that for permeation periods of 12 h or longer, the strain difference between single runs of different permeation time, Fig. 6(a), is of the same magnitude as of the difference between single runs of the permeation period of 24 h, Fig. 6(b). This observation coincides with observations made in a previous study on rabbit muscles.<sup>19</sup> Comparable results were obtained for DP6 and VS55 (not shown in Fig. 6). For the purpose of the current study, most of the data were collected after 24–48 h of permeation, where the difference between 24 and 48 h of permeation can be seen in Fig. 7(b) for 7.05 M DMSO, DP6, and VS55. Note that the muscle specimens are about twice the size of the blood vessel specimens (2 mm × 2 mm × 2 mm versus 1 mm × 2 mm × 2 mm, respectively), and that permeation time is proportional to the specimen's smallest dimension. It follows that the minimum time required for permeation in bovine muscle specimens is longer than the minimum time required for permeation in blood vessel specimens, and that the minimum permeation time of 12 h identified for bovine muscle, is definitely adequate for both tissue types.

Figure 7 presents a summary of thermal strain measurements for (a) goat artery samples after 48 h of permeation, and (b) bovine muscle samples after 24 and 48 h of permeation. It can be seen from Fig. 7(a) that the magnitude of the thermal strain of 7.05M DMSO and DP6, in the absence of biological material, is the higher limit (with a negative sign, due to contraction) to thermal expansion of tissue samples permeated with cryoprotectants. It can further be seen that tissue samples permeated with VS55 show somewhat larger thermal strain at some part of the experimented temperature range. We could not explain this observation, however, given the relatively high data scattering on VS55, the significance of this observation is not clear. Comparable results from bovine muscle samples are shown in Fig. 7(b). For consistency, Fig. 7(b) presents results for 24 h and 48 h of permeation, separately.

An interesting phenomenon, first observed in our previous study,<sup>16</sup> is associated with naturally dissolved gasses in water. Frequently, the thermal strain in the liquid state during rewarming appeared similar to the thermal strain during cooling, but with a constant shift. The dissolved gases (mostly O<sub>2</sub>), do not change the volume of a water sample, and do not affect its thermal expansion in the liquid state. During freezing however, water molecules rearrange in a rigid structures to form crystals, while “pushing away”

the dissolved gas molecules. These gas molecules form small bubbles, which can be easily observed (by the naked eye) in ice cubes. During rewarming, most of the dissolved gases that escaped the liquid during solidification do not return into the liquid, but rather remain in the form of micro-bubbles. Although the overall volume of these bubbles is insignificant compared to the volume of the cooling chamber, the measured parameter here is the change in volume, and not the volume itself. The overall volume of these micro-bubbles is comparable in magnitude to the volume expansion of the cryoprotectant. The constant shift in thermal strain was found in the first cooling/rewarming cycle on a given sample. If the experimentation on the same sample was repeated, this shift in thermal strain disappeared. In order to eliminate the micro-bubble effect in the current study, an extra stage in solution preparation was added, which is freezing the water in liquid nitrogen and rewarming it before the cryoprotectant solutions were prepared. This additional stage eliminated the shift in thermal strain, and increased experimental repeatability. Either way, since the thermophysical property of thermal expansion is the gradient of the thermal strain, and not the thermal strain itself, a strain offset between cooling and rewarming bears no effect on thermal expansion calculations. Although the effect of the presence of micro-bubbles on thermomechanical stress development may be questionable (which deserves further attention), the same effect on the viability of the biological material after rewarming remains unexplored. Hence, it is deemed good practice to prefreeze all cryoprotectant solutions before permeation into biological materials.

## SUMMARY AND CONCLUSIONS

As part of an ongoing effort to characterize the effects of continuum mechanics during cryopreservation, the current study focuses on measuring the thermal expansion of cryoprotective agents, in the presence and absence of biological samples of bovine muscles and goat arteries. The cryoprotectants under investigation are 7.05 M DMSO, DP6, and VS55, with permeation time of up to 48 h. This study focuses on the upper part of the cryogenic temperature range, where the cryoprotectant behaves like a liquid in the relevant cooling rates. Parallel efforts are currently being devoted to measuring thermal expansion during glass transition in biomaterials. Together, these efforts cover the entire relevant cryogenic temperature range to cryopreservation via vitrification.

The device used in this study is a modification of a prototype presented recently, where modifications are related to biological materials handling. High repeatability in strain measurements was obtained for cryoprotectants in the absence of biological samples

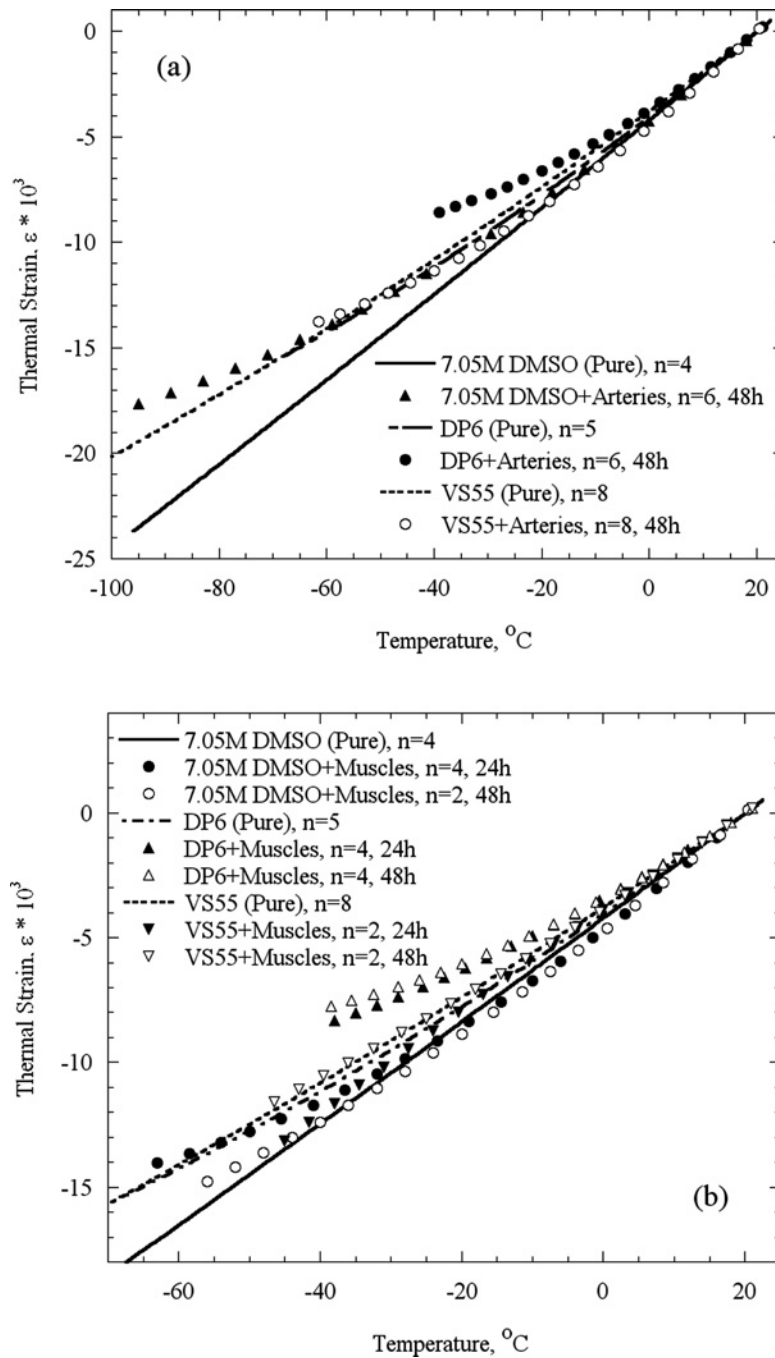


**FIGURE 7.** Summary of thermal strain of artery samples (a), and of bovine muscle samples (b), permeated with 7.05 M DMSO, DP6, and VS55. Best-fit coefficients are listed in Table 1.

after cryoprotectant prefreezing. Somewhat higher scattering of experimental data was observed in the presence of tissue samples permeated with the same cryoprotectant.

Based on thermal strain observations, it is concluded that the presence of tissue samples promotes crystallization (the tissue samples serve as potential nucleation sites). For a

given cryoprotectant in comparable thermal conditions, experiments on bovine muscle samples show higher scattered data than experiments on artery samples. The implication of this observation in continuum mechanics analyses of cryopreserved tissues is that, even if the tissue is cooled at close-to-uniform thermal conditions, mechanical stress may develop due to nonuniform thermal strain distribution.

This effect, as well as other continuum mechanics effects during tissue vitrification, is the subject of continuous effort by this research group.

It is shown in this study that the thermal strain of 7.05 M DMSO and DP6 in the absence of tissue samples is the upper limit, when compared with the thermal strain of artery samples permeated with the same cryoprotectants. The thermal strain of artery samples permeated with 7.05 M DMSO and DP6 is about 75% of the strain of the pure cryoprotectants, when compared at  $-95$  and  $-40^{\circ}\text{C}$ , respectively. Results from VS55 show the opposite trend at some part of the cryogenic temperature range, however, it is not evident that this difference is significant, primarily due to scattering of experimental data. Comparable results with muscle samples are demonstrated for DP6 only, where data are more scattered for bovine muscle samples than for artery samples permeated with the same cryoprotectant.

In order to eliminate the volume change effect associated with the naturally dissolved gasses in the cryoprotectant solution, it is recommended that the solution be prefrozen at least once before introducing it to the biological material. While the role of the dissolved gases in thermomechanical stress development is not yet clear, it may carry an additional damaging effect on the integrity and viability of the biological material.

#### ACKNOWLEDGMENT

This study has been supported in part by NHLBI, grant number R01 HL069944-01A1.

#### REFERENCES

- <sup>1</sup>Almassi, G. H., B. Farahbakhsh, T. Wooldridge, N. J. Rusch, and G. N. Olinger. Endothelium and vascular smooth muscle function in internal mammary artery after cryopreservation. *J. Surg. Res.* 60:355–360, 1996.
- <sup>2</sup>Fahy, G. M., D. R. MacFarlane, C. A. Angell, and H. T. Meryman. Vitrification as an approach to cryopreservation. *Cryobiology* 21:407–426, 1984.
- <sup>3</sup>Fahy, G. M., D. Levy, and S. E. Ali. Some emerging principles underlying the physical properties, biological actions, and utility of vitrification solutions. *Cryobiology* 24:196–213, 1987.
- <sup>4</sup>Fahy, G. M., Biological effects of vitrification and devitrification. In: *The Biophysics of Organ Preservation*, edited by D. E., Pegg, and A. M., Karow, Jr. New York: Plenum Publishing Corp., 1987, pp. 265–297.
- <sup>5</sup>Fahy, G. M., Vitrification. In: *Low Temperature Biotechnology: Emerging Applications and Engineering Contributions*, edited by J. J., McGrath, and K. R., Diller, New York: ASME Press, 1988, pp. 113–146.
- <sup>6</sup>Fahy, G. M., J. Saur, and J. R. Williams. Physical problems with the vitrification of large biological systems. *Cryobiology* 27:492–510, 1990.
- <sup>7</sup>Hunt, C. J., Y. C. Song, E. A. J. Bateson, and D. E. Pegg. Fractures in cryopreserved arteries. *Cryobiology* 31:506–515, 1994.
- <sup>8</sup>Karow, A. M. Biophysical and chemical considerations in cryopreservation. In: *Organ preservation for transplantation*, edited by A. M., Karow, D. E., Pegg, New York: Dekker, 1981, pp. 113.
- <sup>9</sup>Mazur, P. Freezing of living cells: mechanisms and implications. *Am. J. Physiol.* 247:125, 1984.
- <sup>10</sup>Muller-Schweinitzer, E., P. Stulz, H. Striffeler, and W. Haefeli. Functional activity and transmembrane signaling mechanisms after cryopreservation of human internal mammary arteries. *J. Vasc. Surg.* 27:528–537, 1988.
- <sup>11</sup>Nataf, P., P. Hadjiisky, P. Lechat, N. Mougenot, M. Peuchmaurd, R. Gouezo, J. Gerota, C. Cabrol, and I. Gandjbakhch. Effect of cold anoxia and cryopreservation on metabolic and contractile functions of human mammary artery. *Cryobiology* 23:327–333, 1995.
- <sup>12</sup>Pegg, D. E., I. A. Jacobsen, W. J. Armitage, and M. J. Taylor. Mechanisms of cryoinjury in organs. In: *Organ Preservation II*, edited by D. E., Pegg, and I. A., Jacobsen, Edinburgh: Churchill Livingstone, 1979, pp. 132–146.
- <sup>13</sup>Pegg, D. E., Principles of tissue preservation. In: *Progress in Transplantation*, edited by P. J., Morris, and N. L., Tilney, Edinburgh: Churchill Livingstone, 1985, pp. 69–105.
- <sup>14</sup>Pegg, D. E., Ice crystals in tissues and organs. In: *The Biophysics of Organ Preservation*, edited by D. E., Pegg, and A. M., Karow, Jr. New York: Plenum Publishing Corp., 1987, pp. 117–140.
- <sup>15</sup>Pegg, D. E., M. C. Wustemanm, and S. Boylan. Fractures in cryopreserved elastic arteries: mechanism and prevention. *Cryobiology* 33:658–659, 1996.
- <sup>16</sup>Plitz, J., Y. Rabin, and J. Walsh. The effect of thermal expansion of ingredients on the cocktails VS55 and DP6. *Cell Preservation Technology* 2(3):215–226, 2004.
- <sup>17</sup>Rabin, Y., and P. S. Steif. Analysis of thermal stresses around cryosurgical probe. *Cryobiology* 33:276–290, 1996.
- <sup>18</sup>Rabin, Y., and P. S. Steif. Thermal stresses in a freezing sphere and its application to cryobiology. *ASME J. of Appl. Mech.* 65(2):328–333, 1998.
- <sup>19</sup>Rabin, Y., M. J. Taylor, and N. Wolmark. Thermal expansion measurements of frozen biological tissues at cryogenic temperatures. *ASME J. Biomech. Eng.* 120(2):259–266, 1998.
- <sup>20</sup>Rabin, Y., and P. S. Steif. Thermal stress modeling in cryosurgery. *Int. J. Solids and Structures* 37:2363–2375, 2000.
- <sup>21</sup>Rabin, Y., and E. Bell. Thermal expansion measurements of cryoprotective agents. Part I: A new experimental apparatus. *Cryobiology*, 46(3):254–263, 2003.
- <sup>22</sup>Rabin, Y., and E. Bell. Thermal expansion measurements of cryoprotective agents. Part II: Measurements of DP6 and VS55, and comparison with DMSO. *Cryobiology* 46(3):264–270, 2003.
- <sup>23</sup>Rabin, Y., M. J. Michael, J. R. Walsh, S. Baicu, and P. S. Steif. Cryomicroscopy of vitrification, Part I: A prototype and experimental observations on the cocktails VS55 and DP6, *Cryobiology*, submitted.
- <sup>24</sup>Song, Y. C., B. S. Khirabadi, F. G. Lightfoot, K. G. M. Brockbank, and M. J. Taylor. Vitreous cryopreservation maintains the function of vascular grafts. *Nature Biotechnology* 18:296–299, 2000.
- <sup>25</sup>Stanke, F., D. Riebel, S. Carmine, J.-L. Cracowski, F. Caron, J.-L. Magne, and H. Egelhoffer. Functional assessment of human

- femoral arteries after cryopreservation. *J. Vasc. Surg.* 28:273–283, 1998.
- <sup>26</sup>Taylor, M. J. Sub-zero preservation and the prospect of long-term storage of multicellular tissues and organs. In: *Transplantation immunology: clinical and experimental*, edited by R. Y., Calne, Oxford, New York, Tokyo: Oxford University Press, 1984, pp. 360–390.
- <sup>27</sup>Taylor, M. J., Y. C. Song, and K. G. M. Brockbank. Vitrification in tissue preservation: New developments. In: *Life in the Frozen State*, edited by B. J., Fuller, N., Lane, E. E., Benson, CRC Press, New York, 2004.